GS-2014-F101

แบบขออนุมัติหัวข้อและโครงร่างฯ
Request Form for Dissertation/Thesis/I.S. Title and Proposal Approval

บัณฑิตวิทยาลัย มหาวิทยาลัยเชียงใหม่
The Graduate School, Chiang Mai University

วันที่ 20 เดือน พฤศจิกายน พ.ศ. 2562
Date — Month — Year (BE)

ข้าพเจ้า (นาย/~~นาง~~/~~นางสาว~~) นเรนทร์ฤทธิ์ ธนานุศักดิ์   รหัสนักศึกษา 610531046
I am (Mr/Mrs/Ms)   Student Code

นักศึกษาระดับ ☐ ปริญญาเอก ☒ ปริญญาโท ☐ อื่นๆ ....   หมายเลขโทรศัพท์ 083-5154197
studying in   Doctoral Degree   Master's Degree   Other   Telephone No.

หลักสูตร ☒ ปกติ ☐ นานาชาติ ☐ อื่นๆ ....   Email: n.thananusak@gmail.com
Program: Regular   International   Other

สาขาวิชา ดาราศาสตร์   แบบ/~~แผน~~ 2   คณะ วิทยาศาสตร์   มีความประสงค์
Major/Field of Specialization   Type/Plan   Faculty of   would like to request for

ขอเสนอหัวข้อและโครงร่างเพื่อทำ ☒ วิทยานิพนธ์ ☐ การค้นคว้าแบบอิสระ   ในหัวข้อเรื่อง
approval of the Title and Proposal for doing   Dissertation/Thesis   Independent Study   with the Title shown below

(Title in Thai) ฟังก์ชันกำลังส่องสว่างของวัตถุตัวเลือกที่มีเรดชิฟต์สูงในสมัยของการรีไอออไนซ์ (เรดชิฟต์ ≳ 6) ในเขตข้อมูลคอสมิกอีโวลูชันเซอร์เวย์

(Title in English) Luminosity Function of High-redshift z Object Candidates at the Epoch of Reionization (Redshift z ≳ 6) in Cosmic Evolution Survey (COSMOS) Field

โดยได้ ☒ ผ่านเงื่อนไขภาษาต่างประเทศ IELTS คะแนน 5.5 และ การสอบวัดคุณสมบัติ เมื่อ 28/10/2559
has passed Foreign Language Test (TOEFL/IELTS/TEGS, etc - Specify with Score)   and Qualifying Examination on DD/MM/YYYY (BE)

และขอให้ 1. ผศ. ดร. สุวิชา วรรณวิเชียร   เป็น ☒ อาจารย์ที่ปรึกษา ☐ ประธานกรรมการฯ
Under the advice of   as the   Advisor   Advisory Committee Chair

และ 2. ดร. อุเทน แสวงวิทย์   3. ผศ. ดร. ศิรามาศ โกมลจินดา   เป็นกรรมการฯ
and   as Committee Members/Co-advisors

ตามข้อเสนอโครงร่างฯ ที่แนบ จึงเรียนมาเพื่อโปรดอนุมัติและแต่งตั้งคณะอาจารย์ที่ปรึกษาต่อไป
Details shown in the attached proposal and please appoint the proposed Advisor/Advisory Committee

(ลงนาม) .... นักศึกษา
(Signature)   Student

เห็นชอบ

(ลงนาม) .... อาจารย์ที่ปรึกษา
(Signature)   Dissertation/Thesis/I.S. Advisor
(ผศ. ดร. สุวิชา วรรณวิเชียร)
24 / 00 / 62

☒ เห็นชอบโดย กก. ประจำฯ ในการประชุม 13/2562 เมื่อ
Consented by Executive Program Committee on 12/10/2562

ความเห็นอื่น ....
Other comments
(ลงนาม) .... ประธานฯ บ.ศ. คณะ/บว.
(Signature)   Executive Program Chair
(ผู้ช่วยศาสตราจารย์ ดร.จิรัฏฐ์ แสนทน)
รองคณบดีฝ่ายวิชาการ ปฏิบัติการแทน
ประธานกรรมการบัณฑิตศึกษาประจำคณะวิทยาศาสตร์

☒ เห็นชอบโดย กก. สาขาฯ ในการประชุม 8/2562 เมื่อ
Consented by Academic Program Committee on 13/ พย / 62

ความเห็นอื่น ....
Other comments
(ลงนาม) .... ประธานฯ หลักสูตร/สาขา
(Signature)   Academic Program Chair
(ผศ. ดร. ศิรามาศ โกมลจินดา)
24 / 00 / 62

☐ ทราบ
Acknowledged
(ลงนาม) .... คณบดีบัณฑิตวิทยาลัย
(Signature)   Dean of the Graduate School
(....................)
.... / .... / ....

THESIS TITLE AND RESEARCH OUTLINE

1. Student Name and Surname / Code

นายนเรนทร์ฤทธิ์ ธนานุศักดิ์

Narenrit Thananusak

Student Code: 610531046

2. Thesis Title

ฟังก์ชันกำลังส่องสว่างของวัตถุตัวเลือกที่มีเรดชิฟต์สูงในสมัยของการรีไอออไนซ์ (เรดชิฟต์ $\gtrsim 6$) ในเขตข้อมูล คอสมิกอีโวลูชันเซอร์เวย์

Luminosity Function of High-redshift z Object Candidates at the Epoch of Reionization (Redshift $z \gtrsim 6$) in Cosmic Evolution Survey (COSMOS) Field

3. Advisory Committee/Thesis Advisor

Asst. Prof. Dr. Suwicha Wannawichian	Advisor
Dr. Utane Sawangwit	Co-advisor
Asst. Prof. Dr. Siramas Komonjinda	Co-advisor

4. Principles, Theory, Rationale and/or Hypotheses

During redshift (z) ≈ 6, the epoch of reionization (EoR) is understood to be the era that formed the first-generation stars, galaxies or supermassive blackhole (SMBHs). The emitted UV photons from these primordial bright objects ionized the neutral hydrogen in the intergalactic medium (IGM); eventually, this process was widespread entire universe. In recent decades, the EoR studies became interesting topics in observational cosmology, but we still not provided clearer information (i.e. How and when did the first-generation stars or galaxies exactly form, or how did the primordial objects ionize the hydrogen) (Fan, 2012). Since, we can use high-z objects data as the powerful probe to trace back to the EoR, the galaxies luminosity function (LF) investigations place crucial interpretation to constraint on the ionized-photon contributions at that time (Madau & Dickinson, 2014); while the definition of LF is the number density of objects per their absolute brightness per distance interval. The challenges of high-z galaxies ($z \gtrsim 3$) observations are not only the cosmological effect that shifts the UV luminosity to optical or near-infrared wavelengths, but the neutral hydrogen in the IGM absorbs high-z galaxies photons along the line of sight so called "Lyman-break galaxies (LBGs) (Steidel & Hamilton, 1992)."

1

Consequently, our aim is to present the LF from $z \gtrsim 6$ candidates by selecting from LBGs and photometric redshift (photo-z) techniques. We will obtain the dedicated data from the second data release of the Hyper Suprime-Cam Subaru Strategic Program (HSC-SSP DR2) for *riz* wavelength bands (Aihara, et al., 2019). The fourth data release of Ultra-deep Visible and Infrared Survey Telescope for Astronomy (UltraVISTA DR4) in *zYJHK$_S$* wavelength bands (McCracken, et al., 2012). Both ultra-deep surveys overlap on the sky are which are the cosmic evolution survey (COSMOS) field, centered at RA~10h00m28.6s DEC~+2°12'21.0" (Scoville, et al., 2007). Accordingly, we will compare and discuss our results with other works at similar redshift range.

4.1 Brief Cosmic History

When we observe the extremely distance objects, we are looking into the past of our universe. Because, the luminous sources take time to travel. From Hubble-Lemaître law, we can approximate the distance of those objects by observing their redshifted spectra. This redshift is called "cosmological redshift", because the universe is expanding and stretch the very distant objects spectra. Therefore, the study of high-z objects is the way to study the primordial universe.

Around 400,000 years after the Big Bang ($z \sim 1,200$) (Komatsu, et al., 2011), while the universe was expanding, the cosmic temperature dropped to $\sim 3,000$ Kelvins. Such falling temperature allowed electrons (e^-) and protons (p^+) to combine to form the neutral hydrogen (HI) atoms. The combination reaction is $e^- + p^+ \rightarrow HI + \gamma$, where γ is a photon. This era is called "the epoch of recombination." Before this epoch, free electrons and photons from the Big Bang strongly coupled by Thompson scattering reaction, $e^- + \gamma \rightarrow e^- + \gamma$. But after the combination process began, the number of free electrons that used to couple with photons are significantly dropped, which directly effects Thompson scattering rate. Eventually, entire photons decoupled with electrons. The radiation of these primordial photons can pass through to the present universe with their stretching wavelengths by cosmological redshift. Thus, we can observe this radiation so called the "cosmic microwave background (CMB)." After the baryons did not couple with photons due to the recombination anymore, the universe moved toward to the cosmic "dark age." Backward before the recombination era, it is the time that the matter perturbations cannot accrete due to the domination of Big Bang radiation pressure. But in the dark age era, the universe was dominated by matters (i.e. baryons and dark matter). When the gravity force from matters initiated the density fluctuations, it could be the end of the dark age. The dark age ended when the gravitational collapsing of baryons in the primordial dark matter halos, then formed the first-generation (Population-III) stars or galaxies in the large-scale structure (LSS) (Baumann & Daniel, 2018).

The formations of these primordial objects were not just light up the universe again but played a major role on the cosmic chemical transition. Initially, their UV emitted photons ionized the surrounding HI that became to ionized hydrogen (HII). When the number of these objects highly increased and were sufficient in our universe, the fraction of ionized gas drastically growth and widen from the interstellar mediums (ISM) to intergalactic mediums (IGM). Eventually, at the present, the ionized regions extended to entire universe. This era is called, "the epoch of reionization (EoR)." Our current frontiers strongly suggest that the EoR possibly occurs within the redshift range of $z \sim 15 - 6$ and it is the prolonged process (Fan, 2012). Figure 1. illustrates the simulation of reionization evolution as a function of time and redshift. The diagram also shows the EoR's effect, which appears in 21 cm radiative temperatures that equivalent to the HI density.
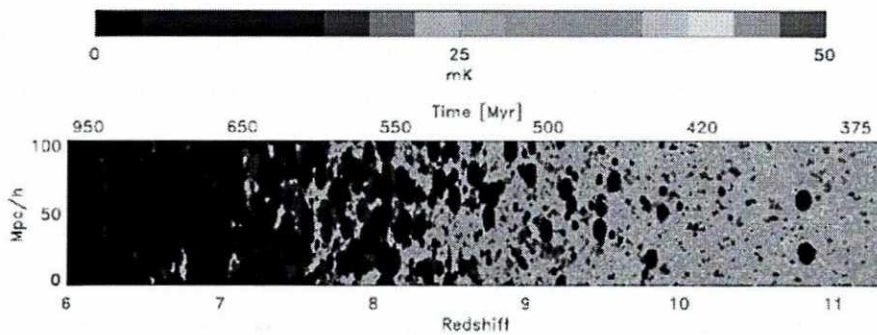

Figure 1. The slice through redshift to 21 cm radiation that equivalent to the HI density. At high-z, the universe mostly consists of HI regions (gray color). Whereas at low-z, the reionization regions (black color) start to appear (Fan, 2012).

4.2 Lyman-break Galaxies (LBGs)

The high-z galaxy observations are the method that focuses on early universe studies. Hence, high-z galaxies are the powerful probes that lead us to better understand their mechanism and evolution back from reionization epoch to the present universe. However, high-z observations are not just be effected by the expanding universe that drastically shifted the wavelengths of sources. The high-level of neutral hydrogen around the ISM or further to IGM absorbed the light from the $z > 3$ galaxies in some regions of spectral energy that have the wavelengths less than the Lyman-alpha (Lyα) line (Fan, 2012). Since, the emitted UV photons from high-z objects give the photon energy that influences the ground state hydrogen atoms in ISM to become excited or ionized. We can calculate the wavelengths that hydrogen absorbs the photon energy, which is specified by Rydberg formula: $\frac{1}{\lambda} = R_H \left(\frac{1}{n_i^2} - \frac{1}{n_f^2} \right)$, where λ, R_H, n_i and n_f are the emitted or absorbed wavelengths, the Rydberg constant (10,973,731.6 m^{-1}), the quantum principal number

of principal number and the quantum principal number of final state, respectively. The wavelength that the neutral hydrogen transition starts to is the Ly-α, when hydrogen with the quantum number $n_i = 1$ absorbs energy then transits the state to $n_f = 2$, whose related energy is equivalent to the wavelength of 1215 Å. The Lyman limit wavelength is 912 Å, which is equivalent to the ionized state of the Hydrogen atom ($n_i = 1 \longrightarrow n_f = \infty$).

Therefore, the challenging is to observe the high$-z$ objects which are shifted to longer wavelength (i.e. from UV to optical, near-infrared or further), and are also absorbed along the line of sight by ISM and IGM. Although, the high-z spectrum might be greatly disturbed, this is the distinctive characteristic that lead us the technique to classify between the low and high reshift objects on observation field. Such technique is called "Lyman-break galaxies" technique. Moreover, due to the high HI density along the line of sight at $z \gtrsim 6$ (closely back to the EoR), the absorption lines are merged and continuity like the 'trough' in the spectrum which is called, "dropout" or "Gunn-Peterson Trough (Gunn & Peterson, 1965)." Figure 2. demonstrates the spectrum of $z \sim 6.0 - 7.1$ quasars, which explicitly indicates the Gunn-Peterson trough. The LBGs key studies are the significant probe that are really important to understand the mechanism of star formation at that time (Fan, 2012).
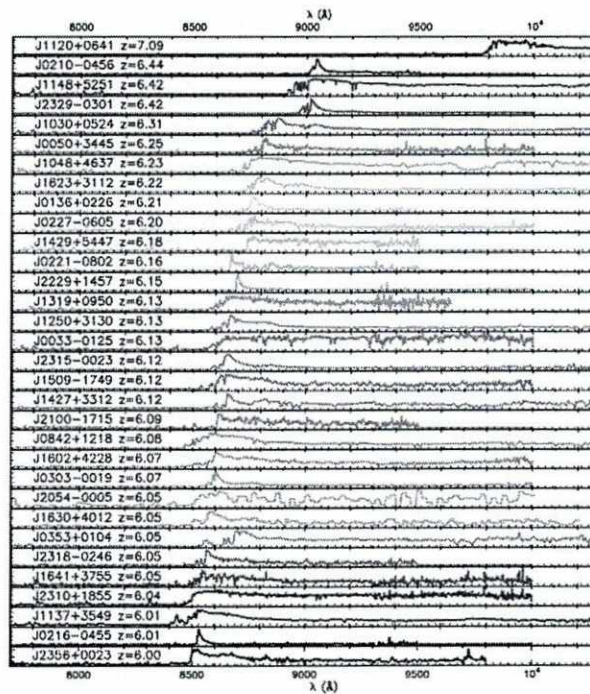

Figure 2. The spectrum of pulbish $z > 6$ quasars that present the stong Lyα absorption or "Gunn-Person trough." Moreover, the quasars spectrum that turn to redder wavelength has higher redshift (Fan, 2012).

4.3 Luminosity Function (LF)

Luminosity function (LF) is defined by the distribution of objects number density as a function of absolute brightness unit per distance interval; i.e. $\phi(M)dM$ and $\phi(L)dL$ are defined by the number density per absolute magnitude (M) and per luminosity (L), respectively. From the definition the LF can be written as:

$$\phi(L) = \frac{n(L)}{V(L)} ,$$

(1)

where $n(L)$ is the number of objects per luminosity and $V(L)$ is the volume of luminosity.

The LF of high-z objects are essentially significant to trace the EoR universe. These key studies are able to: extrapolate the number density of the objects that fainter than the magnitude limit of surveys; trace the cosmic evolution by investigating the number density per brightness as a function of redshift; prove the assumption of isotropic and homogeneous universe by analyzing the LFs in similar distance but different sky areas; and probe the contributions of primordial UV-emitted objects that ionized the IGM during the EoR (Pei, 1995). From subsection 4.4, the $z \gtrsim 3$ objects are strongly absorbed the Ly-α in UV wavelengths spectral region which is called LBGs; the observations on this UV rest-frame are also redshifted to optical or near-infrared windows (Steidel & Hamilton, 1992). Therefore, the UV LF describes the number density of the high-z objects which are obtained from the data in optical/near-IR bands.

4.3.1 Schechter Function

Since, the first-generation stars or galaxies could be collapsed to form by the gravity from the small seed fluctuations in the cold dark matter halos; while, the massive dark matter halos could be rarely formed more than the small halos. After the primordial formations, the small halos hierarchically clustered and becomed enormous clusters in later time (Navarro, et al., 1997). Thus, the number distribution on LF indicates that the bright objects are generally less than faint objects. Nevertheless, due to the magnitude limit of observations, amount of objects that their apparent magnitudes are more than the limit are not detected. Although there are numerous parameters that could describe the shape of luminosity function, it is unlikely completely understood yet. Press-Schecter formalism is one of the appropriate models that describe the concept of cold dark matter cosmological model (Press & Schechter, 1974). Afterwards, in 1976, Paul Schecter applied the function to fit the luminosity function of galaxy cluster so called, "Schecter function." This function in the unit of luminosity is:

$$n(L)dL = \phi^* \left(\frac{L}{L^*}\right)^{\alpha} e^{-L/L^*} \frac{dL}{L^*} ,$$

(2)

where there are three parameters: ϕ^* is a normalisation that can be a number, a number per unit volume or a probability; L and L^* are a luminosity and a characteristic of galaxy luminosity, respectively; α is a slope of faint-part objects that is an observed parameter in the field (i.e. a less number describes a steep trend). The Schechter function has two parts where the L^* is the parameter that cuts off between the bright and the faint population. The $L < L^*$ objects is described by the general faint population, which is defined as the power law function ($\phi \propto L^\alpha$). On the other hand, $L > L^*$ objects is described by the rare bright population, which is defined as the decreased exponential function ($\phi \propto e^{-L}$). Furthermore, the Schechter function can be written as a function of absolute magnitude. The equation is:

$$n(M)dM = 0.4\ln 10\ \phi^* \left[10^{0.4(M^*-M)}\right]^{\alpha+1} \exp\left[-10^{0.4(M^*-M)}\right] dM \,,\tag{3}$$

where M^* is a characteristic of absolute magnitude.

4.4.2 LF Evaluation Method: $1/V_{max}$ estimation

The LF determination on field samples as COSMOS field (Scoville, et al., 2007) that focuses on each similar z −ranges is fundamental of observational cosmology, because it can indicate the population at that time. The most common and simplest method that can estimate the number density is called "$1/V_{max}$" method (Schmidt, 1968; Felten, 1977). To use this method, all observed objects are brighter than the magnitude limit of the surveys. Then use their distances to compute their luminosities (the distances are approximated by photometric-redshift method see 4.6). After that, the LF is formed by the histogram with the bin of their brightness. Unfortunately, there are the "Mamquist bias" that leads the objects which are fainter than the magnitude limit to not be detected. To correct this bias, we can define the volume of surveys by defining the flux limit which is the minimum of flux that the surveys can detect:

$$f_{\text{lim}} = \frac{L}{4\pi d_{\text{max}}^2} \rightarrow d_{\text{max}} = \left[\frac{L}{4\pi f_{\text{lim}}}\right]^{1/2},\tag{4}$$

$$V_{\text{max}} = \frac{4\pi}{3}\left[\frac{L}{4\pi f_{\text{lim}}}\right]^{3/2},\tag{5}$$

where f_{lim} is the flux limit of surveys facilities, d_{max} is the maximum distance that the faintest objects are able to be detected (the distances are approximated by photo metric redshift method) and V_{max} is the maximum volume that depends on the limit flux. The higher luminosity returns larger V_{max} than lower luminosity. Hence, from equation 4, we can find the density of objects by dividing the number of objects in each bin with V_{max} from equation 5. However, this method is unlikely to be a good approximation for nearby objects.

4.5 Photometric Redshift (Photo-z)

Although, the spectroscopic observations are effective and consistent method to measure the redshift. But for high-z objects, their extremely weak fluxes are unlikely detected by spectroscopic surveys and it is not efficient method to determine their distances due to time for operation. One efficient technique is photometric redshift (photo-z) technique. The photo-z procedure approximates the redshift by using the fluxes in multi-wavelengths from photometric data. Such photo-z and LBGs techniques help to filtrates the high-z objects in the selected field from the contamination i.e. spurious sources, red-dwarfs stars or low-z galaxies. After that, we use *hyperz* program to measure the photo-z, which is available on the website http://webast.ast.obs-mip.fr/hyperz. The *hyperz* procedure is to use various spectral energy distribution templates (SEDs) to fit on our observed fluxes and find the best fit by χ^2 minimization (Bolzonella, et al., 2000). The χ^2 minimization equation is defined:

$$\chi^2(z) = \sum_{i=1}^{N_{filters}} \left[\frac{f_{obs,i} - b \cdot f_{temp,i}(z)}{\sigma_i} \right]^2 \tag{6}$$

where f_{obs} is the observed fluxes, f_{temp} is the template fluxes, σ_i is their uncertainties in filter i, and b is a normalization constant.

After the *hyperz* program find the best fit from our samples, the program can approximates numerous outputs i.e. primary best-fit photometric redshift, age, type of objects. The crucial component of photometric redshift is the SED templates which have their own characteristic of spectrum, because it has to comprehend all of the objects in the data for fitting. The SEDs in *hyperz* can be largely distinguished into two types.

4.5.1 Observed SEDs

The *hyperz* contains observed SED set from Coleman, Wu & Weedman (CWW) (Coleman, et al., 1980). Such observed SED is obtained from real UV spectroscopic surveys by Astronomical Netherland Satellites (ANS). The spectral data of every types of nearby galaxies are collected to build the characteristic of different shapes of galaxies. Moreover, the data can be used to estimate the colors and magnitudes of galaxies from nearby to $z = 2$. However, this original SED set did not include the effect of galaxy evolution and have the data only between $400 - 1000 \, \text{Å}$ wavelength; therefore, this SED set are extrapolated by using the averages of Bruzual & Charlot spectrum (Bruzual & Charlot, 1993).

4.5.2 Synthetic SED

The *hyperz* includes synthetic SED set called "Galaxy Isochrones Synthetic Spectral Evolution Library (GISSEL98)" from Bruzual & Charlot (Bruzual & Charlot, 1993). This SED is widespread, due to the good precision fitting for prevalent wavelengths from UV to far-IR, and the possibility of high-z object's' spectral evolution. Such synthetic models are based on the stellar tracks libraries and SEDs are allocated to all stars on the evolutionary tracks. Hence, the Initial Mass Function (IMF) and the Star Formation Rate (SFR) were specified to follow the evolution of the spectrum 2×10^{10} years.

5. Literature Review

5.1 The bright-end of $z \simeq 6$ galaxy LF in COSMOS field from UltraVISTA DR2

The COSMOS field is one of the deep-survey areas that have various surveys overlapping on it, the observations aim to understand back to the primordial universe. The COSMOS field has the area ~ 1.5 deg^2, centered at RA $\sim$ 10h00m28.6s Dec $\sim$ +2°12'21.0" (Scoville, et al., 2007). Bowler et al. (2014) studied the LF that focused on the bright populations with UV rest-frame absolute magnitude (M_{UV}) between -22.7 to -20.5 of $z \simeq 6$ LBGs by selecting the candidates from ultraVISTA DR2 and HSC-SSP DR1 that also overlap on the COSMOS field (Bowler, et al., 2015). They also selected the candidates from UKIRT Deep Sky Survey; UKIDSS (Lawrence, et al., 2007) in the ultra deep survey; UDS fields, with some parts of the data from Subaru XMM-Newton Deep Survey; SXDS (Furusawa, et al., 2008) and VISTA Deep Extragalactic Observations survey; VIDEO (Jarvis, et al., 2013). The catalogs have the data on $rizyYJHK_s$ −bands whose transmission filters are shown in figure 3.
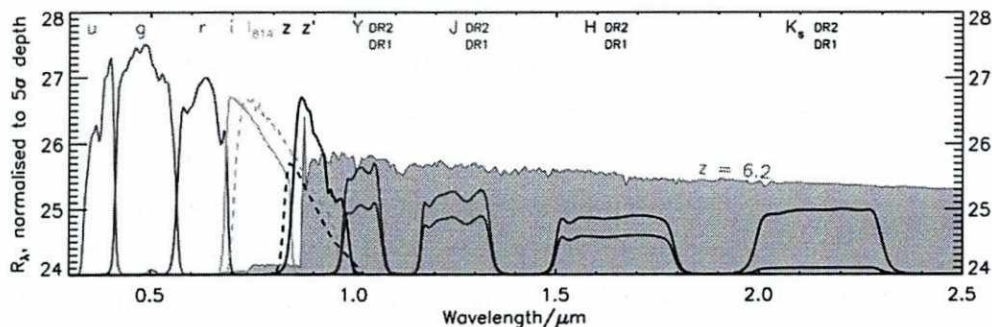

Figure 3. The graph shows the transmission of various filters from ultraVISTA. The $YJHK_s$ filters shows two curves in each filter to describe that the ultraVISTA DR2 data are deeper than DR1. The grey color spectra is the example model of galaxy that is redshifted from Bruzual & Charlot (2003). This example spectra is obviously seen the dropout and is detectable around 0.9 μm to longer wavelengths (Bowler, et al., 2015).

The criteria that they used is to select the data that fainter than the magnitude limit of 26.0 in ultraVISTA DR2 (ultra-deep in COSMOS), and 25.0 in ultraVISTA DR2 (deep) regions in z-band. After that, Bowler et al. (2014) approximated the redshifts of selected candidates by photo-z fitting with the SED templates from Bruzual & Charlot, 2003 and assumed that all candidates with the reddening law from Calzetti, et al., 2000 are on the timescales evolution between 50 Myr -10 Gyr. The selection on high-z LBGs are categorized by the models with the ages from 10 Myr to the universe age at $z = 5$, the total in v-band (A_v) are between 0.0 - 2.0 and the single metallicity (Z) = 0.2 $Z_\odot$, where $Z_\odot$ is the solar metallicity. In contrast, they obtained the contamination model that mainly are the galactic low-z dwarfs which are the red cool stars (spectral types M,L or T) and have the strong absorption in Lyman series, similarly with the LBGs spectrum. This model allows the age from the cosmic age to the present universe, $A_v = 0.0 - 0.6$ and the single $1.0Z_\odot$. The latter model is to exclude the contamination from high-z candidates. Moreover, with χ^2-minimization method, they excluded the objects that has the $\chi^2 > 10.0$ criterion. This works assumed the ΛCDM cosmology with Ω_m, Ω_Λ and H_0 = 0.3, 0.7 and 70 km s^{-1} Mpc^{-1}, respectively and used the AB magnitude system for their LF.

After the candidates selection, the candidates are determined to calculate the LF. The selected samples were also solidly reduced of the contaminants by excluding the candidates which have the signal-to-noise $< 7\sigma$ in z-band. They used the $1/V_{max}$ (Schmidt, 1968) method for calculating the bin of LF as described in section 4.4 . The LF used the UV rest-frame magnitude interval between $-22.625 < M_V < -21.125$ with the 0.25 or 0.5 of binned LF. The LF of this work compared with other previous works are illustrated in fig 4.

These results from this work are found to be consistent with the hierarchical build-up process in the halos of dark matter. However, there were systematic errors in the LF that directly effected the functional fitting. Their UV $z \simeq 6$ LF that is compared to the semi-analytical models of galaxy formations indicated that the medels have over predictied the number density of bright population and have to involve the attenuation up to $A_{1500} \simeq 1.5 - 2.0$ for approving with the models. In our work, we focus on the HSC-SSP DR2 and ultraVISTA DR4 data that have recently been released (Aihara, et al., 2019; McCracken, et al., 2012) for newer and more sophisticated analysis, which located in the COSMOS field.
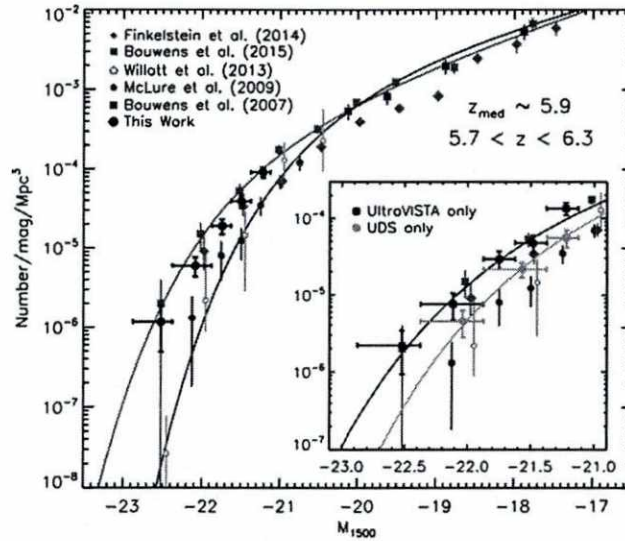
Figure 4. The UV $z \simeq 6$ LF samples, Bowler et al. (2014) works used the data from ultraVISTA/COSMOS and UDS/SXDS are plotted as the black circles. The smaller inset frame shows red circles plots and orange circles for the two different data from ultraVISTA and UDS, respectively. The schechter function is obtained to best fit on each data sets as shown in their individual lines (Bowler, et al., 2015).

5.2 The UV LF Implication

For the $z \sim 7 - 8$ UV LF samples, Bouwens et al. (2011) interpreted their LF which were obtained the data in Hubble ultra-deep field and wide-area early release science field in various topics. Firstly, they discussed the parameters and their uncertainties of Schechter functions in various z −intervals (Bouwens, et al., 2011). The Schechter's parameters are the logarithm of number density ($\log \phi^*$), the characteristic of AB absolute magnitude in UV rest-fram ($M^*_{UV,AB}$) and the faint-end slope (α). Figure 5 presents that there are not crucially different of $z \sim 7 - 8$ LF, both LF are well fit with the Schechter function. Thus, this work indicated that there are no sign of ϕ^* or α evolutions by the contour plots of uncertainties. The implication of LF can be used to describe the galaxy evolution. They converted the luminosity densities to estimate the SFR densities by using the method presented by Maudau et al. (1998) with the Salpeter initial mass function (IMF) in the range $0.1M_\odot - 125M_\odot$, where $M_\odot$ is one solar mass. They found that the limits of SFR densities are 6% for $z \sim 7$ and 4% for $z \sim 8$, while the SFR densities are peak at $z \sim 2 - 3$. Figure 6 illustrates the plot of SFR density (left axis) and luminosity densities (right axis) as a function of redshifts (bottom) and ages in 10^9 years (top).
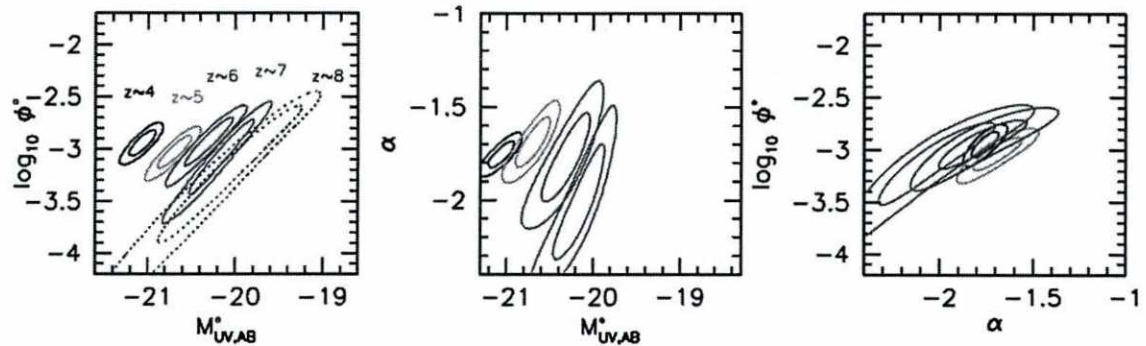
Figure 5. The contour plots of uncertainties in 68% (inner contour) and 95% (outer contour) on Shechter's parameters of UV LF are shown with   in red color dash lines. For lower redshift (, the data for this redshift is not included in the plots. The right panel demonstrates that the number densities as a function of faint-end slope has no evolution base on their uncertainties (Bouwens, et al., 2011).
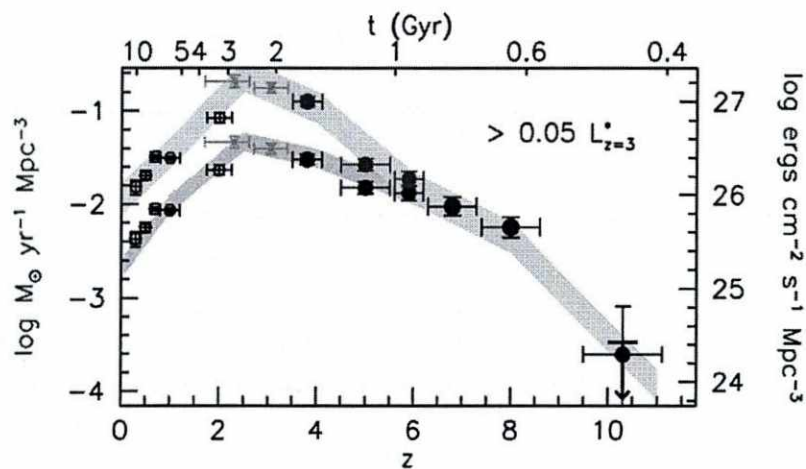

Figure 6. The SFR density as a function of redshfits. The lower trend points and the blue regions are their measurements before dust correction, the latter are after dust correction. The dust correction is assumes to be zero on   . Their work are plotted as blue and red color plot. For more comprehension, they added the   by the data from Reddy & Steidal (2009) and blck squre dots for

6. Research Objectives

6.1 To select the $z \gtrsim 6$ samples in COSMOS field by using LBGs and photo-z techniques, in which data are obtained from the HSC-SSP DR2 and ultraVISTA DR4.

6.2 To estimate the $z \gtrsim 6$ LF and then compare our LF with other works in similar z-range.

7. Usefulness of the Research (Theoretical and/or Applied)

The results will comprehend the understanding of galaxy evolution during the epoch of reionization. It is the time that thought to be when the first-generation of stars or galaxies formed. It can be used to estimate the number of faint objects in our selected field due to the magnitude limit of instruments. Moreover, the data of this work will be useful to compare with other works in the other fields to confirm the postulate of isotropic and homogeneous cosmological model.

8. Research Plan, Methodology and Scope

This work will select the samples to estimate the galaxy UV rest-frame LF in the COSMOS field (Scoville, et al., 2007). The data that we will use are the HSC-SSP DR2 in $rizy$-bands (Aihara, et al., 2019) and the ultraVISTA DR4 in $YJHK_s$ − bands (McCracken, et al., 2012). The technique to select the high-z candidates is the LBGs technique with z-band dropout citeria (e.g. the objects that are fainter than limit magnitude of HSC-SSP in z-band and in shorter regions). The redshifts of previous technique are estimated by photo-z technique by using the *hyper* program (Bolzonella, et al., 2000). The *hyper* procedure is to use the CCW and GIESELS98 SEDs that are contained in the program to find the best-fit on multi-wavelengths data by χ^2 − minimization method. We then select the objects that has percent of primary best-fit probability higher than 70% and has the second best-fit probability lower than 50%. After the selection, the LF will be evaluated by using the $1/V_{max}$ method (Schmidt, 1968; Felten, 1977). Eventually, our LF will be compared with other works that studied in different fields such as Bouwens et al. (2011).

Research plan	Month			
	1-3	4-6	7-10	10-12
Literature survey and literature review	▓			
Prepare for analysis data - studying the structure of catalogs from the surveys - studying the procedure of *hyperz* program	▓			
Select the candidates from LBGs and photo-z techniques		▓		
Calculate the LF from selected candidates		▓		
Compare with other works and discuss		▓		
Recheck all of processes and improve the robustness of samples		▓	▓	
Writing thesis and publication			▓	▓
Defense Examination				▓

9. Research Location

9.1 Department of Physics and Materials Science, Faculty of Science, Chiang Mai University, Chiang Mai, Thailand

9.2 National Astronomical Research Institute of Thailand (NARIT), Chiang Mai, Thailand

10. Research Duration

12 months

11. Bibliography

Aihara, H. et al., 2019. Second Data Release of the Hyper Suprime-Cam Subaru Strategic Program. *eprint arXiv:1905.12221,* May.p. 24.

Baumann & Daniel, 2018. TASI Lectures on Primordial Cosmology. *arXiv preprint arXiv:1807.03098,* 9 July.

Bolzonella, M., Miralles, J.-M. & Pelló, R., 2000. Photometric redshifts based on standard SED fitting procedures. *Astronomy and Astrophysics,* November, Volume 363, pp. 476-492.

Bouwens, R. J. et al., 2011. Ultraviolet Luminosity Functions from 132 z ~ 7 and z ~ 8 Lyman-break Galaxies in the Ultra-deep HUDF09 and Wide-area Early Release Science WFC3/IR Observations. *The Astrophysical Journal,* August, 737(2), p. 90.

Bowler, R. A. A. et al., 2015. The galaxy luminosity function at z ≃ 6 and evidence for rapid evolution in the bright end from z ≃ 7 to 5. *Monthly Notices of the Royal Astronomical Society,* 452(2), pp. 1817-1840.

Bruzual, G. & Charlot, S., 1993. Spectral evolution of stellar populations using isochrone synthesis. *Astrophysical Journal,* March, 405(2), pp. 538-553.

Bruzual, G. & Charlot, S., 2003. Stellar population synthesis at the resolution of 2003. *Monthly Notices of the Royal Astronomical Society,* October, 344(4), pp. 1000-1028.

Calzetti, D. et al., 2000. The Dust Content and Opacity of Actively Star-forming Galaxies. *The Astrophysical Journal,* April, 533(2), pp. 682-695.

Coleman, G. D., Wu, C.-C. & Weedman, D. W., 1980. Colors and magnitudes predicted for high redshift galaxies. *Astrophysical Journal Supplement Series,* July, Volume 43, pp. 393-416.

Fan, X., 2012. Observations of the first light and the epoch of reionization. *Research in Astronomy and Astrophysics,* 12(8), pp. 865-890.

Felten, J. E., 1977. Study of the luminosity function for field galaxies. *Astronomical Journal,* November, Volume 82, pp. 861-878.

Furusawa, H. et al., 2008. The Subaru/XMM-Newton Deep Survey (SXDS). II. Optical Imaging and Photometric Catalogs. *The Astrophysical Journal Supplement Series,* May, 176(1), pp. 1-18.

Gunn, J. E. & Peterson, B. A., 1965. On the Density of Neutral Hydrogen in Intergalactic Space.. *Astrophysical Journal,,* November, Volume 142, pp. 1633-1636.

Jarvis, M. J. et al., 2013. The VISTA Deep Extragalactic Observations (VIDEO) survey. *Monthly Notices of the Royal Astronomical Society,* January, 428(2), pp. 1281-1295.

Komatsu, E. et al., 2011. Seven-year Wilkinson Microwave Anisotropy Probe (WMAP) Observations: Cosmological Interpretation. *The Astrophysical Journal Supplement,* February, 192(2), p. 47.

Lawrence, A. et al., 2007. The UKIRT Infrared Deep Sky Survey (UKIDSS). *Monthly Notices of the Royal Astronomical Society,* August, 379(4), pp. 1599-1617.

Madau & Dickinson, 2014. Cosmic Star-Formation History. *Annual Review of Astronomy and Astrophysics,* August, Volume 52, pp. 415-486.

McCracken, H. J. et al., 2012. UltraVISTA: a new ultra-deep near-infrared survey in COSMOS. *Astronomy & Astrophysics,* August, Volume 544, p. 11.

McLure, R. J. et al., 2010. Galaxies at z = 6-9 from the WFC3/IR imaging of the Hubble Ultra Deep Field. *Monthly Notices of the Royal Astronomical Society,* April, 403(2), pp. 960-983.

Navarro, J. F., Frenk, C. S. & White, S. D. M., 1997. A Universal Density Profile from Hierarchical Clustering. *The Astrophysical Journal,* December, 490(2), pp. 493-508.

Pei, Y. C., 1995. The luminosity function of quasars. *The Astrophysical Journal,* January, 438(2), pp. 623-631.

Press, W. H. & Schechter, P., 1974. Formation of Galaxies and Clusters of Galaxies by Self-Similar Gravitational Condensation. *The Astrophysical Journal,* February, Volume 187, pp. 425-438.

Schmidt, M., 1968. Space Distribution and Luminosity Functions of Quasi-Stellar Radio Sources. *Astrophysical Journal,* February, Volume 151, p. 393.

Scoville, N. et al., 2007. The Cosmic Evolution Survey (COSMOS): Overview. *The Astrophysical Journal Supplement Series,* September, 172(1), pp. 1-8.

Steidel, C. C. & Hamilton, D., 1992. Deep imaging of high redshift QSO fields below the Lyman limit. I - The field of Q0000-263 and galaxies at z = 3.4. *Astronomical Journal,* September, Volume 104, pp. 941-949.

12. Thesis Advisors

The undersigned have read and approved this thesis proposal and have agreed to act as the Thesis Advisory Committee in the respective capacities mentioned below.

(Signed)..Chairperson

(Asst. Prof. Dr. Suwicha Wannawichian)

(Signed)..Co-advisor

(Dr. Utane Sawangwit)

(Signed).. Co-advisor

(Asst. Prof. Dr. Siramas Komonjinda)

หนังสือยินยอมมอบทรัพย์สินทางปัญญา
Letter of Consent to Consign Intellectual Properties

ที่ .... / ....
Ref. No. (issued by the Graduate School)

บัณฑิตวิทยาลัย มหาวิทยาลัยเชียงใหม่
The Graduate School, Chiang Mai University

วันที่ .... เดือน .... พ.ศ. 2562
Date   Month   Year (BE)

ข้าพเจ้า (นาย/~~นาง~~/~~นางสาว~~) นเรนทร์ฤทธิ์ ธนานุศักดิ์
I am (Mr/Mrs/Ms)

รหัสนักศึกษา 610531046
Student Code

นักศึกษามหาวิทยาลัยเชียงใหม่ ระดับ ☐ ปริญญาเอก ☒ ปริญญาโท ☐ อื่นๆ ....
Student of Chiang Mai University studying in   Doctoral Degree   Master's Degree   Other

☒ หลักสูตรปกติ ☐ หลักสูตรนานาชาติ ☐ อื่นๆ ....
Regular Program   International Program   Other

หมายเลขโทรศัพท์ 083-5154197
Telephone No.

สาขาวิชา ดาราศาสตร์
Major/Field of Specialization

แบบ/~~แผน~~ 2
Type/Plan

ตกลงยินยอมมอบ ลิขสิทธิ์ สิทธิบัตร อนุสิทธิบัตร สิทธิในงานประดิษฐ์ ความลับทางการค้า และทรัพย์สินทาง
ปัญญาอื่นๆ ในวิทยานิพนธ์หรือการค้นคว้าแบบอิสระที่ได้รับอนุมัติตามหัวข้อเรื่องดังนี้ (ภาษาไทยและอังกฤษ)

agree to consign Copyright, Patent, Petty Patent, Patent of Invention, Trade Secret and other Intellectual Properties in the

approved Dissertation/Thesis/Independent Study as specified in the following Title (in Thai and English)

(Title in Thai) ฟังก์ชันกำลังส่องสว่างของวัตถุตัวเลือกที่มีเรดชิฟต์สูงในสมัยของการรีไอออไนซ์ (เรดชิฟต์ $\gtrsim 6$)
ในเขตข้อมูลคอสมิกอีโวลูชันเซอร์เวย์

(Title in English) Luminosity Function of High-redshift z Object Candidates at the Epoch of Reionization
(Redshift z $\gtrsim$ 6) in Cosmic Evolution Survey (COSMOS) Field

ให้แก่มหาวิทยาลัยเชียงใหม่ตลอดอายุการคุ้มครองตามกฎหมายที่เกี่ยวข้องกับทรัพย์สินทางปัญญา
to Chiang Mai University throughout the Legal Protection of any involved Intellectual Property Law

(ลงนาม) .... นักศึกษา
(Signature)   Student
(......นเรนทร์ฤทธิ์ ธนานุศักดิ์......)

(ลงนาม) .... อาจารย์ที่ปรึกษา
(Signature)   Dissertation/Thesis/I.S. Advisor
(......ผศ. ดร. สุวิชา วรรณวิเชียร......)

(ลงนาม) .... คณบดีบัณฑิตวิทยาลัย
(Signature)   Dean of the Graduate School
(..)

IELTS™

Test Report Form

	ACADEMIC

NOTE Admission to undergraduate and post graduate courses should be based on the ACADEMIC Reading and Writing Modules.
GENERAL TRAINING Reading and Writing Modules are **not** designed to test the full range of language skills required for academic purposes.
It is recommended that the candidate's language ability as indicated in this Test Report Form be re-assessed **after two years** from the date of the test.

Centre Number	TH001	Date	28/OCT/2017	Candidate Number	013377

Candidate Details

Family Name	THANANUSAK
First Name	NARENRIT
Candidate ID	1549900432278

Date of Birth	09/01/1996	Sex (M/F)	M	Scheme Code	Private Candidate

Country or Region of Origin	
Country of Nationality	THAILAND
First Language	THAI

Test Results

Listening	5.5	Reading	6.0	Writing	5.5	Speaking	5.5	Overall Band Score	5.5	CEFR Level	B2

Administrator Comments

	Centre stamp	Validation stamp
	●● BRITISH ●● COUNCIL	IELTS

	Administrator's Signature	
Date	09/11/2017	Test Report Form Number	17TH013377THAN001A

●● BRITISH ●● COUNCIL   idp IELTS AUSTRALIA   CAMBRIDGE ENGLISH Language Assessment Part of the University of Cambridge

The validity of this IELTS Test Report Form can be verified online by recognising organisations at http://ielts.ucles.org.uk